JOURNAL OF VIROLOGY, Apr. 1994, p. 2521–2528
0022-538X/94/$04.00+0

Vol. 68, No. 4

An Apoptosis-Inhibiting Gene from a Nuclear Polyhedrosis Virus Encoding a Polypeptide with Cys/His Sequence Motifs

MARK J. BIRNBAUM,[1,2]† ROLLIE J. CLEM,[1] AND LOIS K. MILLER[1,2]*

Department of Genetics[1] and Department of Entomology,[2] University of Georgia, Athens, Georgia 30602

Received 29 September 1993/Accepted 9 December 1993

Two different baculovirus genes are known to be able to block apoptosis triggered upon infection of *Spodoptera frugiperda* cells with *p35* mutants of the insect baculovirus *Autographa californica* nuclear polyhedrosis virus (Ac*M*NPV): *p35* (P35-encoding gene) of Ac*M*NPV (R. J. Clem, M. Fechheimer, and L. K. Miller, Science 254:1388–1390, 1991) and *iap* (inhibitor of apoptosis gene) of *Cydia pomonella* granulosis virus (CpGV) (N. E. Crook, R. J. Clem, and L. K. Miller, J. Virol. 67:2168–2174, 1993). Using a genetic complementation assay to identify additional genes which inhibit apoptosis during infection with a *p35* mutant, we have isolated a gene from *Orgyia pseudotsugata* NPV (Op*M*NPV) that was able to functionally substitute for Ac*M*NPV *p35*. The nucleotide sequence of this gene, Op-*iap*, predicted a 30-kDa polypeptide product with approximately 58% amino acid sequence identity to the product of CpGV *iap*, Cp-IAP. Like Cp-IAP, the predicted product of Op-*iap* has a carboxy-terminal C3HC4 zinc finger-like motif. In addition, a pair of additional cysteine/histidine motifs were found in the N-terminal regions of both polypeptide sequences. Recombinant *p35* mutant viruses carrying either Op-*iap* or Cp-*iap* appeared to have a normal phenotype in *S. frugiperda* cells. Thus, Cp-IAP and Op-IAP appear to be functionally analogous to P35 but are likely to block apoptosis by a different mechanism which may involve direct interaction with DNA.

The ability of cells to undergo apoptotic cell death in response to viral infection and the ability of viruses to block cellular apoptosis constitute a virus-host interaction which is crucial in determining the outcome of virus infection at both the cellular and organismal levels (4, 22, 34). Because apoptosis is also involved in a wide variety of normal and abnormal organismal processes, including tissue homeostasis, immune system function, embryonic development, and cancer (31), the molecular pathways leading to apoptosis are important to define.

Large DNA-containing viruses are proving to be valuable sources of genes which block apoptosis. Some members of the families *Adenoviridae*, *Baculoviridae*, and *Herpesviridae* have genes involved in blocking cellular apoptosis or programmed cell death during infection (2, 3, 6, 13, 25, 34) or share homology (24, 26) with *bcl-2*, a mammalian proto-oncogene which blocks normal apoptosis when overexpressed (17, 33). Adenovirus E1B proteins are thought to abrogate the function of *p53* (7, 34), a tumor suppressor which accumulates in response to DNA damage (23), arresting the cell cycle at G_1/S for DNA repair (18, 19) and possibly triggering apoptosis when DNA damage is severe (7). Thus far, baculoviruses appear to use genes distinctively different from those of mammalian viruses to block apoptosis. Characterizing these genes and their function(s) is likely to provide insight into the pathways governing this evolutionarily conserved process.

Two different baculovirus genes, *p35* and *iap*, block apoptosis induced after infection of *Spodoptera frugiperda* cells (SF-21) with *p35* mutants of *Autographa californica* nuclear polyhedrosis virus (Ac*M*NPV) (3, 6). Ac*M*NPV *p35* mutants, such as vAcAnh (also known as the annihilator), induce widespread apoptosis in SF-21 cells between 12 and 24 h postinfection (3). Premature cell death by apoptosis results in the shutoff of all protein synthesis, a 100- to 1,000-fold decrease in budded virus production, and the complete absence of occlusion bodies (3, 4, 15). The predicted sequence (10) of the *p35* product, P35, reflects no obvious homology to other sequences in GenBank.

Our interest in searching for apoptosis-inhibiting genes in baculoviruses other than Ac*M*NPV was stimulated by the observation that the *Orgyia pseudotsugata* NPV (Op*M*NPV) genome, which is largely colinear with the Ac*M*NPV genome (1), appears to lack a *p35* homolog (11, 21). Although the genes flanking Ac*M*NPV *p35* and its upstream neighbor *p94* (10) are similarly positioned in Op*M*NPV, these two genes are not present in this position of the Op*M*NPV genome, and no hybridization to Op*M*NPV DNA was observed with Ac*M*NPV *p35* DNA as a probe (11).

With the expectation of locating distantly related homologs of *p35*, we developed a genetic complementation assay to identify apoptosis-blocking genes in which SF-21 cells are cotransfected with vAcAnh and the test baculovirus DNA and transfected cells are subsequently monitored for occluded virus production. Several baculovirus DNAs, including Op*M*NPV DNA and *Cydia pomonella* granulosis virus (CpGV) DNA, were able to complement the *p35* defect in this assay. We first examined the more distantly related CpGV genome and discovered that a single CpGV gene, Cp-*iap* (inhibitor of apoptosis), was able to block apoptosis in vAcAnh-infected cells (6). The product of Cp-*iap*, Cp-IAP, has no sequence homology to the Ac*M*NPV *p35* gene product, P35. Cp-IAP may be a DNA binding protein, on the basis of the presence of a C-terminal zinc finger-like motif, referred to as a C3HC4 motif, which is also found in a number of proteins encoded by virus regulatory genes (e.g., herpes simplex virus ICP0 and Ac*M*NPV *ie-n*), proto-oncogenes (e.g., *mel-18* and PML), insect developmental regulatory genes [e.g., *su(z)2* and *psc*] (5), and other genes encoding DNA-interactive proteins (9, 29). A homolog of Cp-*iap* also exists in the Ac*M*NPV genome, but this homolog, Ac-*iap*, is nonfunctional in the complementation assay (6).

In this study, we found that Op*M*NPV has a gene homolo-

* Corresponding author. Mailing address: Department of Entomology, University of Georgia, Athens, GA 30602. Phone: (706) 542-2294. Fax: (706) 542-2279. Electronic mail address: miller@bscr.uga.edu.

† Present address: Department of Cell Biology, University of Massachusetts Medical School, Worcester, MA 01655.

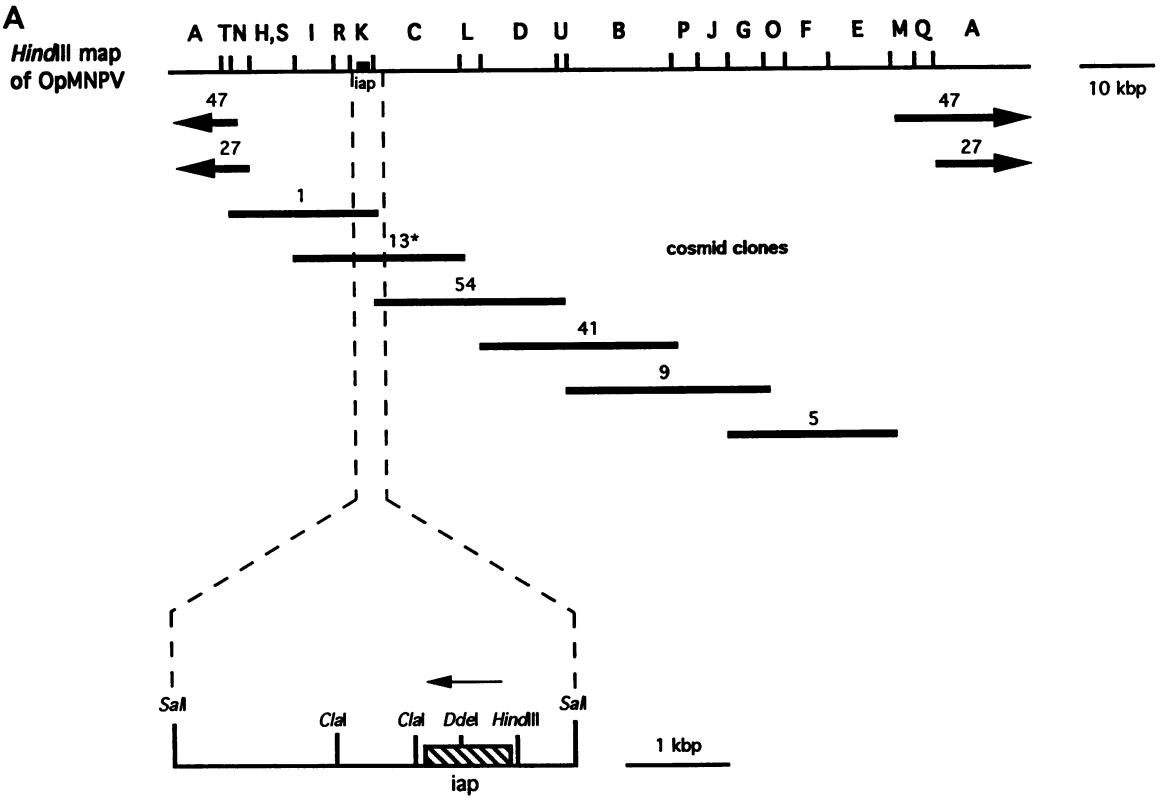

B

```
                                                                  TaqI      HindIII
   1 GTTCCGGTTCTCGCGCATCACGAGCAATAAGCGTTATCATTTTAGATTACAAATTATCAAGATAGCGAATTGCTTATATTCGACGCGACAAGCTTCGTGT  100

 101 TGTCAGAAGCCGCGGGTGAGCGCTCGCGCGCGTTGCAGAATGAGCTCCCGAGCAATTGGCGCGCCGCAAGAAGGCGCAGACATGAAAAACAAAGCCGCGC  200
   1                                                 M  S  S  R  A  I  G  A  P  Q  E  G  A  D  M  K  N  K  A  A  R   21

 201 GTCTCGGCACGTACACCAATTGGCCCGTCCAGTTTTTGGAGCCGAGCCGCATGGCCGCCAGCGGGTTCTACTACTTGGGCCGCGGCGACGAGGTGCGCTG  300
  22   L  G  T  Y  T  N  Y  P  V  Q  F  L  E  P  S  R  M  A  A  S  G  F  Y  Y  L  G  R  G  N  E  V  R  C   54

 301 CGCGTTTTGCAAGGTAGAGATTACGAATTGGGTAAGGGGCGACGACCCGGAAACGGACCACAAGCGGTGGGCGCCGCAGTGTCCGTTTGTGCGCAACAAC  400
  55   A  F  C  K  V  E  I  T  N  W  V  R  G  D  D  P  E  T  D  H  K  R  W  A  P  Q  C  P  F  V  R  N  N   87

 401 GCGCACGACACGCCACACGACCGCGCCCCGCCGGCGCGGTCGGCGGCCGCGCACCCGCAGTATGCCACGGAAGCCGCGCGTTTGCGCACCTTTGCGGAGT  500
  88 A  H  D  T  P  H  D  R  A  P  P  A  R  S  A  A  A  H  P  Q  Y  A  T  E  A  A  R  L  R  T  F  A  Q  W  121

 501 GGCCCCGCGGGTTGAAACAGCGGCCCGAAGAGTTGGCCGAGGCCGGATTCTTTTACACTGGCCAGGGCGACAAGACGCGGTGCTTTTGCTGCGACGGCGG  600
 122   P  R  G  L  K  Q  R  P  E  E  L  A  E  A  G  F  F  Y  T  G  Q  G  D  K  T  R  C  F  C  C  D  G  G  154

 601 TCTGAAGGATTGGGAACCCGACGACGCGCCGTGGCAGCAACACGCCCGCTGGTACGACCGCTGCGAGTACGTGCTGCTCGTCAAGGGCCGCGACTTTGTG  700
 155   L  K  D  W  E  P  D  D  A  P  W  Q  Q  H  A  R  W  Y  D  R  C  E  Y  V  L  L  V  K  G  R  D  F  V   187
            DdeI
 701 CAGCGGGTGATGACTGAGGCGTGTGTGGTTCGCGACGCGGACAACGAACCGCACATTGAGCGGCCGGCCGTTGAAGCGGAGGTGGCGGATGACCGGCTGT  800
 188 Q  R  V  M  T  E  A  C  V  V  R  D  A  D  N  E  P  H  I  E  R  P  A  V  E  A  E  V  A  D  D  R  L  C   221

 801 GCAAGATTTGCCTCGGCGCCGAAAAGACCGTGTGCTTTGTGCCCTGCGGGCACGTGGTGGCGTGCGGCAAGTGCGCTGCGGGCGTGACCACGTGCCCCGT  900
 222   K  I  C  L  G  A  E  K  T  V  C  F  V  P  C  G  H  V  V  A  C  G  K  C  A  A  G  V  T  T  C  P  V   254

 901 TTGCCGCGGTCAGTTAGACAAAGCGGTGCGCATGTACCAAGTGTAACAATAAAACACAAATTTGTTCAAGGTGTTTAATAGCGTCACTAAACTTGTAATA  1000
 255   C  R  G  Q  L  D  K  A  V  R  M  Y  Q  V  *                                                        268
       TaqI
1001 TCGATTAATAAATGCGTTTGCGTTTACAAACAAATGAAGTTTCTATGTCTTCCTCCTTTTCTTCAGATTCGCGTTCCAGTTGGGCACGTAAGCCCCGCGT  1100

1101 ACCGCCTTGTAAACGGTGGAGTTGCTTTCCATCACATTAAACTTGTCCACGCCGCTGTTCTTGTCAAACACCGAAAACGGCGTTTTCGTGTACGGTGTGA  1200

1201 CGCTGTCGGGCGGGGGCACCTGGTTGTCGTTGTAAATTTCGCGCAAAGTAAACCGTGCGTGGTCCAGCAGCCCCGCGAGTTGCTTCTCGGTTAAATCTAG  1300

1301 CCCGATTTTCGCGACCATTGGCTCAACAATTTTGACAAACTGGTCGCCAATGTGGCAAAACAGCTCGTTTATAGCCGTTGTGTTGG                1386
```

FIG. 1. Genomic, cosmid, and subclone maps of Op*M*NPV as well as the nucleotide sequence of Op-*iap*. (A) *Hin*dIII map of the Op*M*NPV genome is shown at the top (21). The thick bars beneath the map represent overlapping cosmid clones used in the complementation assay. The map at the bottom shows restriction sites surrounding the *iap* ORF, which is represented by the cross-hatched box; the arrow above the box indicates the direction of the ORF. (B) Nucleotide sequence of a 1.4-kb active fragment of clone 13 containing *iap*. Below the DNA sequence is the predicted amino acid sequence of IAP. Key restriction potential regulatory sites are indicated. A late transcriptional start site (ATAAG), early TATA box, and polyadenylation signals downstream of the ORF are underlined. The C3HC4 motif is double underlined.

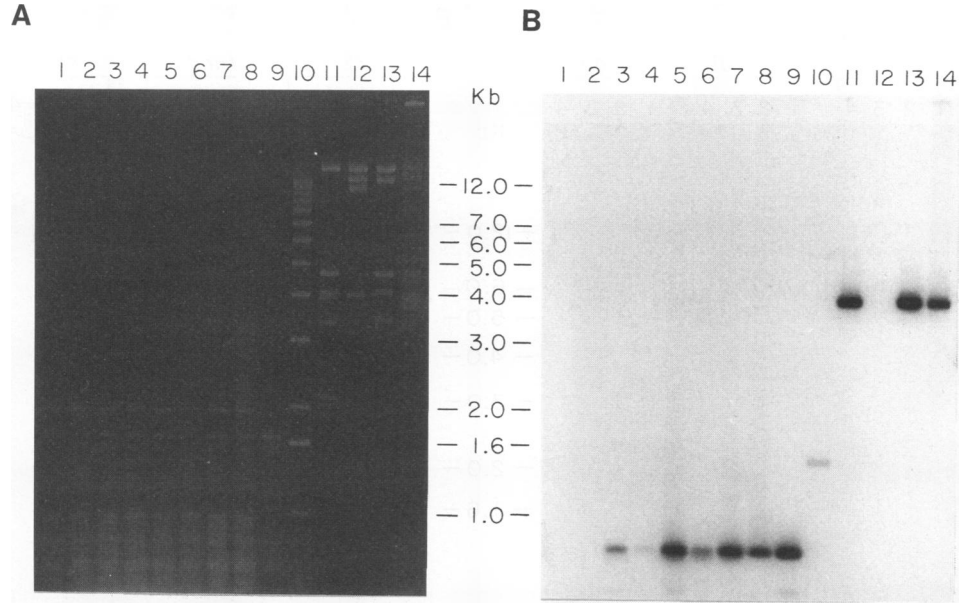

FIG. 2. Analysis of Op-*iap* in *iap*-rescued recombinants of vAcAnh. Restriction endonuclease-digested DNA from the ethidium bromide-stained agarose gel (A) was Southern blotted, hybridized to a 0.9-kb ^{32}P-labeled *Taq*I fragment containing the *iap* ORF (see Fig. 1B), and subjected to autoradiography (B). Lanes 1 through 9 contain DNAs digested with *Taq*I. Lanes: 1, wt Ac*M*NPV; 2, vAcAnh; 3 through 8, vOpIAPR-6 through vOpIAPR-11, respectively; 9, cosmid clone 13; 10, standard DNA ladder. Lanes 11 through 14 are DNAs digested with *Hin*dIII. Lanes: 11 through 13, cosmid clones 1, 54, and 13, respectively; 14, Op*M*NPV genomic DNA. The sizes of standard DNA markers are indicated in the center.

gous to Cp-*iap*, which was able to block vAcAnh-induced apoptosis in SF-21 cells. The Op*M*NPV homolog, Op-*iap*, was in a genomic position roughly equivalent to the position of the Ac-*iap* homolog and was more closely related to Cp-*iap* than to Ac-*iap*. In addition to the C-terminal C3HC4 motif, all three IAPs contain two tandemly repeated Cys/His motifs.

MATERIALS AND METHODS

Viruses and insect cells. Wild-type (wt) Ac*M*NPV (L-1) and recombinant viruses (vASB6-1 and vAnhR11) were propagated in cell lines derived from either *S. frugiperda* IPLB-SF-21 (SF-21) cells (32) or *Trichoplusia ni* TN-368 cells (16), and titers were determined as described previously (6, 27). The mutant vAcAnh was propagated in TN-368 cells only, and its titer was determined. Cells were maintained at 27°C in TC-100 medium supplemented with 10% fetal bovine serum and 0.26% tryptose broth by standard methods (27).

DNA cloning, sequencing, and analysis. Cosmid clones, generated by cloning partially digested *Hin*dIII fragments (21) and spanning the entire genome, were kindly provided by George Rohrmann (Oregon State University, Corvallis). Only cosmid 13 showed activity in the complementation assay (Fig. 1A). An active 3.9-kb *Sal*I-*Pst*I fragment from cosmid 13 was gel purified, subcloned into the *Sal*I-*Pst*I site of pBluescript KS+, and analyzed further. After digestion of the *Sal*I-*Pst*I fragment with *Hin*cII, an active 3.2-kb fragment was further subcloned into the *Eco*RV site of pBluescript KS+. Deletion clones were generated in both directions with exonuclease III and mung bean nuclease (14) and were assayed with the complementation assay, revealing an active 1.4-kb subclone (pOpiap). Subclones were sequenced in both directions by the dideoxy chain termination method and were analyzed with the Intelligenetics and Genetics Computer Group packages (8).

Complementation assay and isolation of recombinant viruses. DNA (1 to 2 μg each) of vAcAnh and test DNA (i.e., Op*M*NPV DNA, cosmid DNA, or plasmid subclones) were cotransfected into SF-21 cells (6). Three to 4 days later, the plates were visually screened by light microscopy. Plates with cells containing occlusion bodies were scored as positive. Recombinant viruses were isolated by plaque purification of budded viruses released from three independent cotransfections of vAcAnh DNA with either the subclone containing the 3.2-kb fragment described above or pOpiap. The recombinants were further purified by two rounds of plaque purification in SF-21 cells before characterization.

Metabolic labeling of infected cells. Protein pulse-labeling of infected cells was carried out as previously described (4, 27) with minor modifications. Briefly, either SF-21 or TN-368 cells (10^6) were infected at a multiplicity of infection of 20 PFU per cell (as assayed in TN-368 cells) or mock infected. After 1 h, the inoculum was replaced with TC-100 (time zero). Two hours before each time point, the cells were resuspended in medium, centrifuged at 1,000 × *g* for 5 min, and resuspended in TC-100 medium lacking supplements, methionine, and cysteine and placed at 27°C. One hour before each time point, the cells were centrifuged again, and the medium was replaced with 0.5 ml of methionine-deficient medium containing 25 μCi of Tran^{35}S-label (>1,000 Ci/mmol [ICN]). At the time point, the cells were centrifuged, the radioactive medium was removed, and the cell pellets were washed, lysed, and stored at −80°C (27). These lysates were analyzed by sodium dodecyl sulfate-polyacrylamide gel electrophoresis (SDS-PAGE) (20) and autoradiography (27).

Nucleotide sequence accession number. The nucleotide sequence presented in this report has been submitted to GenBank and was assigned the number L224564.

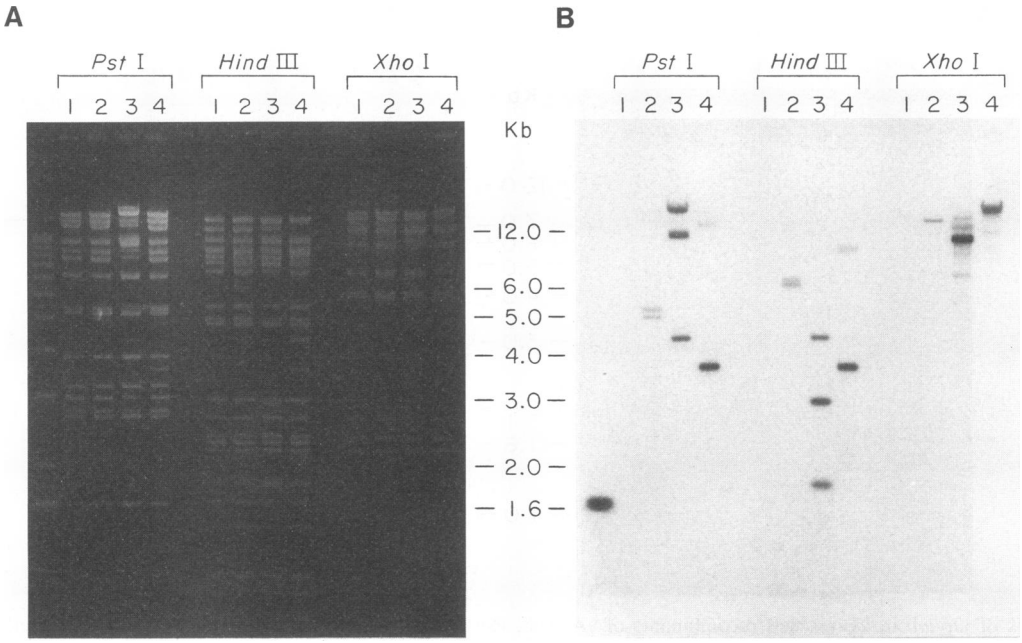

FIG. 3. Localization of *iap* insertions in *iap*-rescued recombinants of vAcAnh. (A) Ethidium bromide-stained DNA restriction fragments after agarose gel electrophoresis. (B) DNA was Southern blotted, hybridized to a 0.9-kb ^{32}P-labeled *Taq*I fragment containing only the *iap* ORF, and subjected to autoradiography. Viral DNA (3 μg) was digested with *Pst*I, *Hin*dIII, or *Xho*I as indicated. Within each group, lane 1 is vAcAnh DNA, lane 2 is vOpIAPR-9, lane 3 is vOpIAPR-10, and lane 4 is vOpIAPR-11. The sizes of the DNA standard markers are indicated in the center.

RESULTS

Mapping and sequencing of an Op*M*NPV gene complementing an Ac*M*NPV *p35* mutant, vAcAnh. Cotransfection of vAcAnh and Op*M*NPV genomic DNA resulted in polyhedral occlusion body formation. Control experiments with either viral DNA transfected individually did not produce polyhedra (data not shown). Thus, a gene or genes in the Op*M*NPV genome could functionally substitute for *p35*. To identify the complementing gene, overlapping cosmid DNAs encompassing the entire Op*M*NPV genome (21) were individually cotransfected along with vAcAnh DNA (Fig. 1A). Only cosmid 13 displayed activity in our assay. Two adjacent cosmid clones, 1 and 54, completely overlapped clone 13 but were negative in the assay, suggesting that the expression of the gene responsible for rescue required sequences spanning the *Hin*dIII site separating clones 1 and 54.

To further define the gene responsible for rescue, subclones of cosmid 13 were tested for complementation. A 3.2-kb *Hin*cII subclone displayed apoptosis-inhibiting activity, and selected deletions of this clone were tested in the complementation assay (see Materials and Methods). One subclone, pOpiap, contained an active 1.4-kb insert, which was sequenced (Fig. 1B).

Computer analysis of the sequence revealed an open reading frame (ORF) capable of encoding a 30-kDa polypeptide (Fig. 1B) sharing 58% amino acid identity with Cp-IAP. Cotransfection assays with several other subclones indicated that this ORF was essential to the rescuing activity of pOpiap (data not shown). Like Cp-IAP, the Op*M*NPV IAP (Op-IAP) has a C3HC4 finger motif at its carboxy terminus.

To determine the orientation and location of Op-*iap* with respect to the restriction map, Southern blots of *Hin*dIII-digested Op*M*NPV DNA (Fig. 2A) were hybridized to a 0.9-kb *Taq*I probe encompassing the entire *iap* ORF (Fig. 2B). This *Taq*I fragment hybridized to the Op*M*NPV *Hin*dIII-K fragment (Fig. 2, lane 14) and to cosmid clones 1 and 13 (Fig. 2, lanes 11 and 13), but it did not hybridize to cosmid 54 (lane 12). A *Hin*dIII site is located approximately 50 nucleotides upstream of the putative translational start site of the 30-kDa ORF and is close to the upstream *Taq*I site. The inserts in cosmids 1 and 54 are separated in the Op*M*NPV genome by a *Hin*dIII site (21). Collectively, the data indicate that Op-*iap* is located at the left end of *Hin*dIII-K and would be expected to be transcribed in the leftward (counterclockwise) direction with respect to the Op*M*NPV map (Fig. 1A). Because the *Hin*dIII site is located between the translational start site of the *iap* ORF and two putative transcriptional regulatory signals, a late consensus TAAG sequence at −112 bp and a putative early TATA box at −64 bp from the ATG, it is likely that the lack of activity of cosmid 1, which contains the intact *iap* ORF, is due to the separation of the *iap* ORF from these 5′ regulatory sequences. We confirmed this by testing a subclone of Op-*iap* truncated at the *Hin*dIII site in the complementation assay; the subclone did not result in formation of polyhedra. The region 3′ of the ORF contains two AATAAA sequences which may serve as polyadenylation signals for *iap* transcripts.

Characterization of vAcAnh-Op*M*NPV *iap* recombinant virus DNA. Cotransfection of vAcAnh DNA with clones containing Op-*iap* resulted in the presence of viruses with an occlusion-positive phenotype in the extracellular media. Six independent recombinants were characterized: three were isolated from vAcAnh cotransfection with pOpiap, and the other three were isolated with the plasmid containing the 3.2-kb *iap*-containing insert. To show that each of the recombinants contained an intact *iap* ORF, genomic DNA from these recombinants was digested with *Taq*I, Southern blotted, and hybridized to the 0.9-kb *Taq*I fragment comprising the entire Op-*iap* ORF (Fig. 2). While viral DNAs isolated from wt Ac*M*NPV and vAcAnh did not hybridize to the probe (Fig. 2B, lanes 1 and 2), all six recombinant DNAs contained the 0.9-kb

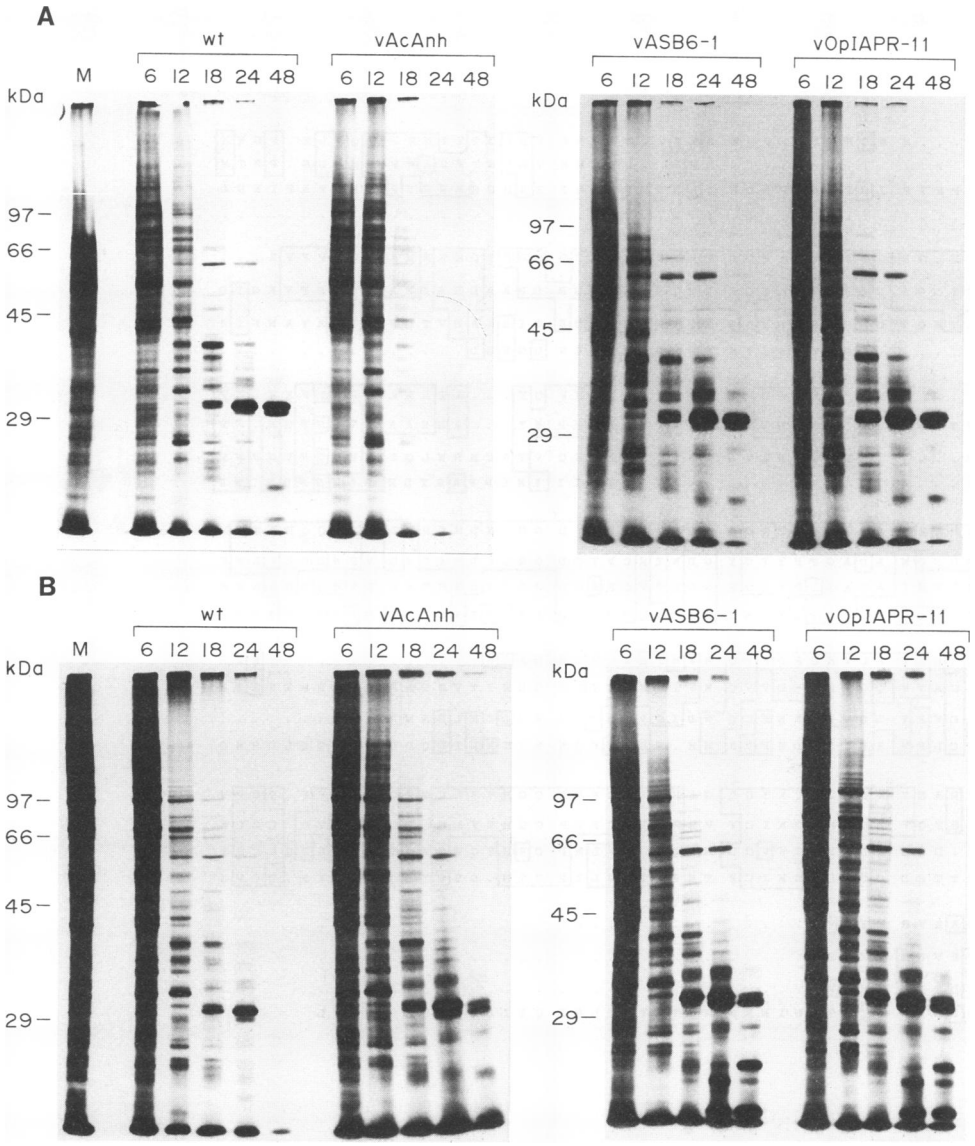

FIG. 4. Kinetics of protein synthesis in cells infected with *iap*-containing recombinants. SF-21 cells (A) or TN-368 cells (B) were infected with wt Ac*M*NPV, vAcAnh, vASB6-1 (a recombinant rescued with Cp-*iap*), or vOpIAPR-11 (a recombinant rescued with Op-*iap*). At selected times (in hours, as shown above the lanes), cells were pulse-labeled and then lysed. Samples were subjected to SDS-PAGE followed by autoradiography. Mock-infected cells (lane M) were treated in parallel as a control. The positions of the molecular mass markers are shown on the left.

fragment (Fig. 2B, lanes 3 to 8), showing that this region remained intact in the recombinants. It is not known why lanes 3, 4, and 6 show less hybridization to the probe DNA; it is likely that these viruses are genetically unstable (see below).

The sites of Op-*iap* integration into the vAcAnh genome were studied by digesting DNA of the three pOpiap-derived recombinants with selected restriction endonucleases (Fig. 3A), which were Southern blotted and hybridized to the 0.9-kb *Taq*I fragment (Fig. 3B). In two recombinants (vOpIAPR-9 and vOpIAPR-10), a complex but reproducible pattern of bands, some of which were submolar, suggested that the recombinants had more than one copy of *iap*. In vOpIAPR-10 (lane 3), the intensities of both the *Hin*dIII-I and *Pst*I-E fragments were decreased, indicating the presence of one or more inserts in the region between 33 and 38 map units; however, the submolar nature of the bands suggested genomic instability and/or persisting impurity of the virus despite three plaque purifications. In vOpIAPR-9 (lane 2), the probe hybridized weakly to new submolar bands in the *Pst*I and *Hin*dIII digests and to a large fragment in the *Xho*I pattern, possibly *Xho*I-C, -D, or -E. Recombinant vOpIAPR-11 DNA (lane 4) displayed alterations in *Hin*dIII-B1 and the *Xho*I-B fragments, indicating a single *iap* insertion between 68 and 75 Ac*M*NPV map units.

Kinetics of protein synthesis in cells infected with *p35* mutant Op-*iap*$^+$ and *p35* mutant Cp-*iap*$^+$ recombinants. Protein synthesis profiles of vOpIAPR-11 and vASB6-1, a recombinant derived from cotransfections of vAcAnh and Cp-*iap* (6), were compared with those from the parent vAcAnh and wt Ac*M*NPV (Fig. 4). In SF-21 cells, the rate, nature, and quantity of protein synthesized in cells infected with either recombinant were virtually indistinguishable from that observed in wt

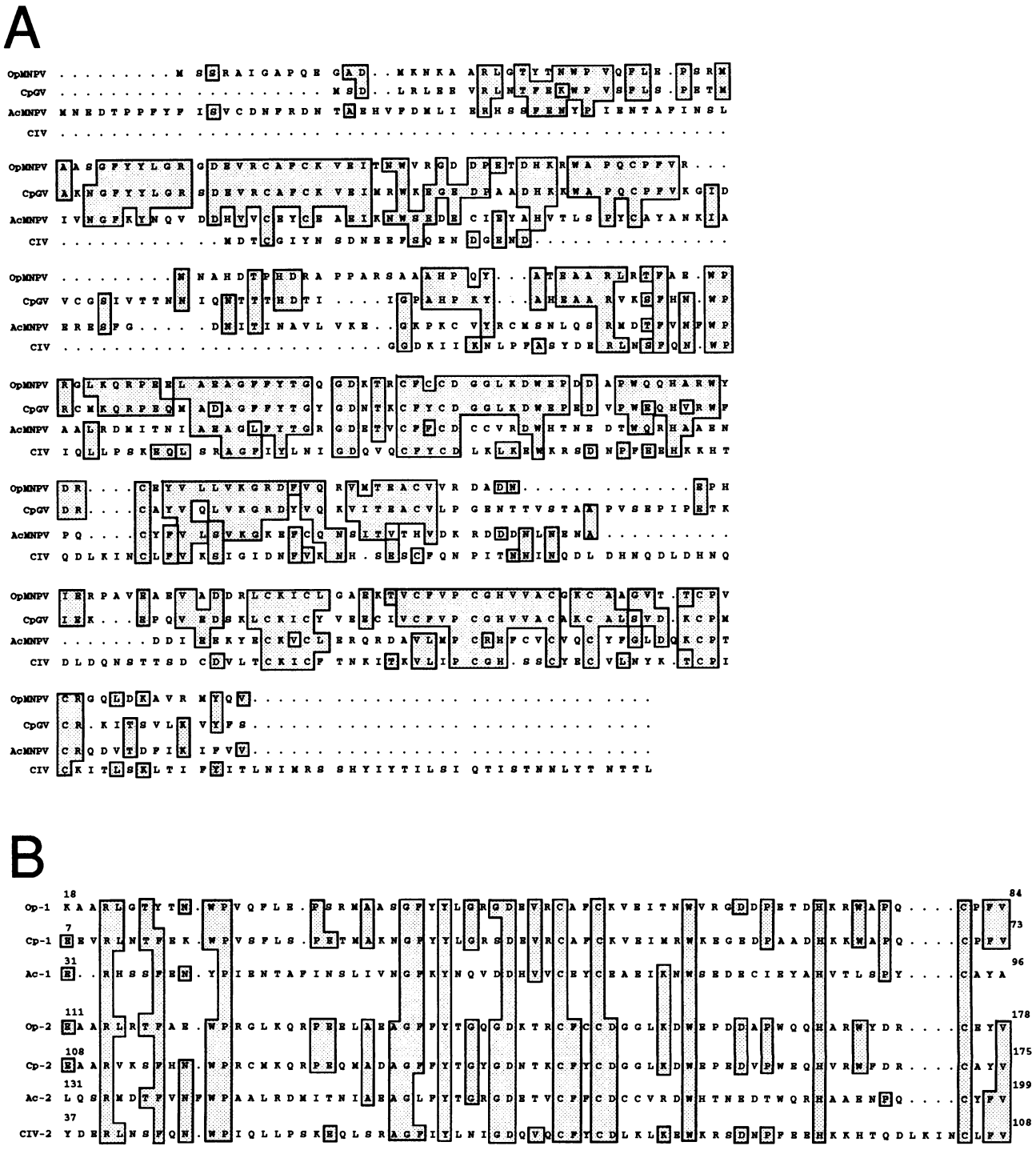

FIG. 5. Sequence alignments of known *iap* homologs. (A) Alignment of the predicted amino acid sequences from the *iap* homologs of Op*M*NPV, CpGV, Ac*M*NPV, and Chilo iridescent virus (CIV). Identical residues are enclosed in shaded boxes, and dots indicate gaps introduced to optimize the alignment. The CIV-IAP nucleotide sequence (12) was frameshifted in two places to obtain the amino acid sequence shown. The alignment was carried out with the Genetics Computer Group PILEUP computer program (8). (B) Alignment of the conserved and repeated amino acid sequences (BIR motifs) found at the N-terminal end of the ORFs. The sequences are compared both among and within the different *iap* homologs. Identical residues conserved in four or more of the sequences are enclosed in shaded boxes. Dots indicate gaps introduced to optimize the alignment. Numbers above the amino acid sequence designate the location of these residues within each corresponding IAP homolog. The first BIR motifs within the Op-*iap*, Cp-*iap*, and Ac-*iap* homologs are indicated as Op-1, Cp-1, and Ac-1, respectively; the second BIR repeats within these *iap* homologs are indicated as Op-2, Cp-2, Ac-2, and CIV-2, respectively.

Ac*M*NPV infections (Fig. 4A). As expected (4, 15), vAcAnh displayed protein synthesis profiles characteristic of early viral infection through 12 h, but protein synthesis diminished as the cells completed apoptosis (4). In TN-368 cells (Fig. 4B), a cell line that does not undergo apoptosis upon infection with vAcAnh, all four viruses showed similar patterns, except that both recombinants expressed higher quantities of several low-molecular-weight proteins than were observed in the wt Ac*M*NPV or vAcAnh protein profiles at 24 and 48 h postinfection. The identity of these peptides was not determined, but they are likely to be breakdown products of polyhedrin. The significance of this observation is not clear; the appearance and quantity of these peptides varied among experiments. The 48-h lane in the wt Ac*M*NPV infection in TN-368 cells shown in Fig. 4B was apparently mishandled during this particular experiment; Ac*M*NPV normally synthesizes significant quantities of polyhedrin at this time.

DISCUSSION

We identified a gene of Op*M*NPV which blocks apoptosis induced during infection of SF-21 cells with Ac*M*NPV mutants lacking functional *p35*. This gene, Op-*iap*, is a homolog of both Cp-*iap* and Ac-*iap*. Op-*iap* and Ac-*iap* appear to be located in similar positions on the relatively colinear genomic maps of Op*M*NPV and Ac*M*NPV, although the correspondence of genes flanking Op-*iap* has not been determined. Op-IAP shares 58% amino acid identity with Cp-IAP but only 28% identity with Ac-IAP, which is functionally inactive in the complementation assay. All three IAP homologs possess a C3HC4 motif (Fig. 5A [specifically $CX_2CX_{11}CXHX_3CX_2CX_{7-8}CPXCR$, where X is any amino acid]) at their carboxyl terminus. This motif is a subset of a more general C3HC4 motif ($CX_2CX_{10-27}CXHX_{2-3}CX_2CX_{5-16}CPXC$) found in approximately 30 other proteins (5), one of which is known to have DNA binding properties. Unlike most of the proteins in this group, the C3HC4 motifs of the IAPs are C terminal rather than N terminal and have a central $CXHX_3CX_2C$ sequence rather than $CXHX_2CX_2C$. C-terminal C3HC4 motifs are also found in the gene encoding peroxisome activating factor (30) and the *Drosophila neuralized* (*neu*) gene which is involved in restricting the number of neural progenitor cells during embryonic neurogenesis (28).

Two tandem repeats of the sequence $GX_2YX_4DX_3CX_2CX_6WX_9HX_{6-10}C$ are present in the N-terminal and central portion of baculovirus IAPs (Fig. 5B). We have named the repeat unit a BIR (baculovirus *iap* repeat) motif; the spacing of cysteines and histidine within the BIR suggests the possibility of metal ion coordination and nucleic acid binding. Additional sequence identities can be found if Ac-*iap*, which is inactive in the assay, is excluded from the comparison. The Chilo iridescent virus homolog, CIV-*iap* (12), is not complete but appears to have at least one BIR motif as well as the C3HC4 motif. The activity of this gene in our assay has not been tested.

Consistent with the apparent nonhomologous integration of Cp-*iap* into vAcAnh (6), Op-*iap* appeared to integrate at multiple sites in the genome of Ac*M*NPV. The sequence identity between Ac-*iap* and the other baculovirus *iaps* may not be enough to favor recombination at this site. Alternatively, the Ac-*iap iap* homolog may have an additional function. Since Op*M*NPV appears to lack a *p35* homolog, it may rely solely on Op-*iap* to block apoptosis. Further genetic analysis of baculovirus *iaps* and *p35* is likely to provide insight into the molecular mechanism(s) of apoptosis.

ACKNOWLEDGMENTS

We are indebted to George Rohrmann for the Op*M*NPV cosmid library. We also appreciate the assistance and advice of Moyra Robson, Steve Hilliard, Bergmann Ribeiro, Jeanne McLaughlin, Russell Eldridge, David O'Reilly, Yong Hong Li, Timothy Morris, Lorena Pasarrelli, Louise McNitt, Karen Hutchinson, and Albert Lu.

This work was supported in part by Public Health Service grant AI23719 from the National Institute of Allergy and Infectious Diseases to L.K.M., by NIH postdoctoral fellowship GM13589 to M.J.B., and by NIH predoctoral training grant GM07103 to R.J.C.

ADDENDUM IN PROOF

The amino acid sequence in Fig. 1B is incorrect in three locations: residue 28 should be W instead of Y, residue 50 should be D instead of N, and residue 120 should be E instead of Q.

REFERENCES

1. **Blissard, G. W., and G. F. Rohrmann.** 1990. Baculovirus diversity and molecular biology. Annu. Rev. Entomol. **35:**127–155.
2. **Chou, J., and B. Roizman.** 1992. The $\gamma_1$34.5 gene of herpes simplex virus 1 precludes neuroblastoma cells from triggering total shutoff of protein synthesis characteristic of programmed cell death in neuronal cells. Proc. Natl. Acad. Sci. USA **89:**3266–3270.
3. **Clem, R. J., M. Fechheimer, and L. K. Miller.** 1991. Prevention of apoptosis by a baculovirus gene during infection of insect cells. Science **254:**1388–1390.
4. **Clem, R. J., and L. K. Miller.** 1993. Apoptosis reduces both the in vitro replication and the in vivo infectivity of a baculovirus. J. Virol. **67:**3730–3738.
5. **Clem, R. J., and L. K. Miller.** Induction and inhibition of apoptosis by insect viruses. *In* L. D. Tomei (ed.), Apoptosis II. The molecular basis of cell death, in press. Cold Spring Harbor Laboratory Press, Plainview, N.Y.
6. **Crook, N. E., R. J. Clem, and L. K. Miller.** 1993. An apoptosis-inhibiting baculovirus gene with a zinc finger-like motif. J. Virol. **67:**2168–2174.
7. **Debbas, M., and E. White.** 1993. Wild-type p53 mediates apoptosis by E1A, which is inhibited by E1B. Genes Dev. **7:**546–554.
8. **Devereux, J. D., P. Haeberli, and O. Smithies.** 1984. A comprehensive set of sequence analysis programs for the VAX. Nucleic Acids Res. **12:**387–395.
9. **Freemont, P. S., I. M. Hanson, and J. Trowsdale.** 1991. A novel cysteine-rich sequence motif. Cell **64:**483–484.
10. **Friesen, P. D., and L. K. Miller.** 1987. Divergent transcription of early 35- and 94-kilodalton protein genes encoded by the *Hin*dIII K genome fragment of the baculovirus *Autographa californica* nuclear polyhedrosis virus. J. Virol. **61:**2264–2272.
11. **Gombart, A. F., G. W. Blissard, and G. F. Rohrmann.** 1989. Characterization of the genetic organization of the Hind-III M region of the multicapsid nuclear polyhedrosis virus of Orgyia-pseudotsugata reveals major differences among baculoviruses. J. Gen. Virol. **70:**1815–1828.
12. **Handermann, M., P. Schnitzler, A. Rosen-Wolff, K. Raab, K.-C. Sonntag, and G. Darai.** 1992. Identification and mapping of origins of DNA replication within the DNA sequences of the genome of insect iridescent virus type 7. Virus Res. **6:**19–32.
13. **Henderson, S., M. Rowe, C. Gregory, D. Croom-Carter, F. Wang, R. Longnecker, E. Kieff, and A. Rickinson.** 1991. Induction of *bcl-2* expression by Epstein-Barr virus latent membrane protein 1 protects infected B cells from programmed cell death. Cell **65:** 1107–1115.
14. **Henikoff, S.** 1984. Unidirectional digestion with exonuclease III creates targeted breakpoints for DNA sequencing. Gene **28:**351–359.
15. **Hershberger, P. A., J. A. Dickson, and P. D. Friesen.** 1992. Site-specific mutagenesis of the 35-kilodalton protein gene encoded by *Autographa californica* nuclear polyhedrosis virus: cell line-specific effects on virus replication. J. Virol. **66:**5525–5533.
16. **Hink, W. F.** 1970. Established insect cell line from the cabbage looper, Trichoplusia ni. Nature (London) **226:**466–467.
17. **Hockenberry, D., G. Nunez, C. Milliman, R. D. Schreiber, and S.**

Korsmeyer. 1990. Bcl-2 is an inner mitochondrial membrane protein that blocks programmed cell death. Nature (London) **348:**334–336.

18. **Kastan, M. B., O. Onyekwere, D. Sidransky, B. Vogelstein, and R. W. Craig.** 1992. Participation of p53 protein in the cellular response to DNA damage. Cancer Res. **51:**6304–6311.
19. **Kuerbitz, S. J., B. S. Plunkett, W. V. Walsh, and M. B. Kastan.** 1992. Wild-type p53 is a cell cycle checkpoint determinant following irradiation. Proc. Natl. Acad. Sci. USA **89:**7491–7495.
20. **Laemmli, U. K.** 1970. Cleavage of structural proteins during the assembly of the head of bacteriophage T4. Nature (London) **227:**680–685.
21. **Leisy, D. J., G. F. Rohrmann, and G. S. Beaudreau.** 1984. Conservation of genome organization in two multicapsid nuclear polyhedrosis viruses. J. Virol. **52:**699–702.
22. **Levine, B., Q. Huang, J. T. Isaacs, J. C. Reed, D. E. Griffin, and J. M. Hardwick.** 1993. Conversion of lytic to persistent alphavirus infection by the *bcl-2* cellular oncogene. Nature (London) **361:** 739–742.
23. **Maltzman, W., and L. Czyzyk.** 1984. UV irradiation stimulates levels of p53 cellular tumor antigen in nontransformed mouse cells. Mol. Cell. Biol. **4:**1689–1694.
24. **Marchini, A., B. Tomkinson, J. I. Cohen, and E. Kieff.** 1991. BHRF1, the Epstein-Barr virus gene with homology to Bcl-2, is dispensable for B-lymphocyte transformation and virus replication. J. Virol. **65:**5991–6000.
25. **Martin, J. M., D. Veis, S. J. Korsmeyer, and B. Sugden.** 1993. Latent membrane protein of Epstein-Barr virus induces cellular phenotypes independently of expression of Bcl-2. J. Virol. **67:** 5269–5278.
26. **Neilan, J. G., Z. Lu, C. L. Afonso, G. F. Kutish, M. D. Sussman, and D. L. Rock.** 1993. An African swine fever virus gene with similarity to the proto-oncogene *bcl-2* and the Epstein-Barr virus gene *BHRF1*. J. Virol. **67:**4391–4394.
27. **O'Reilly, D. R., L. K. Miller, and V. A. Luckow.** 1992. Baculovirus expression vectors: a laboratory manual. W. H. Freeman and Company, New York.
28. **Price, D. B., Z. Chang, R. Smith, S. Bockheim, and A. Laughon.** 1993. The Drosophila neuralized gene encodes a C3H4 zinc finger. EMBO J. **12:**2411–2418.
29. **Schatz, D. G., M. A. Oettinger, and D. Baltimore.** 1989. The V(D)J recombination activating gene, RAG-1. Cell **59:**10–21.
30. **Shimozawa, N., T. Tsukamoto, Y. Suzuki, T. Orii, Y. Shirayoshi, T. Mori, and Y. Fujiki.** 1992. A human gene responsible for Zellweger Syndrome that affects peroxisome assembly. Science **255:** 1132–1135.
31. **Tomei, L. D., and F. O. Cope (ed.).** 1991. Apoptosis I. The molecular basis of cell death. Cold Spring Harbor Laboratory Press, Plainview, N.Y.
32. **Vaughn, J. L., R. H. Goodwin, G. J. Tompkins, and P. McCawley.** 1977. The establishment of two cell lines from the insect Spodoptera frugiperda (Lepidoptera: Noctuidae). In Vitro **13:**213–217.
33. **Vaux, D. L., I. L. Weissman, and S. K. Kim.** 1992. Prevention of programmed cell death in Caenorhabditis elegans by human bcl-2. Science **258:**1955–1957.
34. **White, E., P. Sabbatini, M. Debbas, W. S. M. Wold, D. I. Kusher, and L. R. Gooding.** 1992. The 19-kilodalton adenovirus E1B transforming protein inhibits programmed cell death and prevents cytolysis by tumor necrosis factor α. Mol. Cell. Biol. **12:**2570–2580.